International Journal on Interactive Design and Manufacturing (IJIDeM) (2023) 17:3025–3042
https://doi.org/10.1007/s12008-023-01350-4

ORIGINAL PAPER

# Parametric analysis and optimization of aluminium and SS 204 material using micro-EDM system

**Pritam Pain**[1] · **Goutam Kumar Bose**[1] · **Dipankar Bose**[2]

Received: 24 January 2023 / Accepted: 18 April 2023 / Published online: 11 May 2023


**Abstract**
A Micro EDM machining process is proposed here to machine Aluminium (Grade 201) and SS204 work materials where the material removal rate and the overcut phenomenon are investigated while changing four different control parameters, including voltage (V), duty factor (DF), frequency (F), and tool diameter (Td). Initially, an Analysis of Variance (ANOVA) has been carried out to determine the influence of control parameters on the responses. The effects are shown on the interaction plot of the variables. Next, the Genetic algorithm is used to optimize dual responses. From GA a pool of globally optimal solutions is predicted. Therefore we need to converge to a specific set of parametric combinations that will satisfy the contradictory responses. Then Grey Relational Analysis (GRA) is used to determine the pool of global optima to a single set of process parameters that will simultaneously comply with the responses. The outcome of experiments with the specified set of parameters has been compared to validate the results as mathematically obtained. AL is machined at 49-V voltage, 84% Duty Factor, 18 Hz frequency, and 0.90 mm tool diameter to achieve the highest MRR and lowest OC. In cutting SS204 material, maximum MRR and Minimum OC is achieved at 41-V voltage, 70% Duty Factor, 15 Hz frequency, and 0.90 mm tool diameter.

**Keywords** Micro electric discharge machining · Cuckoo search algorithm · Genetic algorithm · Material comparison

## 1 Introduction

Micro EDM (Electrical Discharge Machining) is a non-traditional machining process that uses a series of electrical sparks to erode or cut material from a workpiece. The process is especially useful for machining complex shapes, intricate patterns, and micro-sized features in hard materials such as metals, ceramics, and composites. A micro EDM system typically consists of a power supply, a dielectric fluid system, a tool electrode, a workpiece, and a control system. The power supply generates a high voltage electrical pulse that is delivered to the tool electrode, which is typically made of a conductive material such as copper or tungsten. The tool electrode is brought close to the workpiece, and the electrical pulse causes a spark to jump across the gap between the electrode and the workpiece. This spark generates a high temperature that melts and vaporizes a small amount of material from the workpiece. The dielectric fluid system is used to control the spark and cool the workpiece. It also serves to flush away the eroded material from the gap between the electrode and the workpiece. The control system monitors and adjusts the various parameters of the EDM process, such as the pulse duration, voltage, current, and frequency. Micro EDM systems are commonly used in industries such as aerospace, medical, and electronics, where there is a need for precision machining of micro-sized components. They can also be used for micro-drilling, micro-milling, and micro-welding applications.

Complex 3D modules and rigid tools can be precisely cut with a very smooth surface finish using this new machining technique known as micro-EDM. The process of micro-EDM involves sparking the workpiece and tool in the dielectric medium. No matter how strong or hard the material is, it can still be machined [1]. Bose and Pain [2] used an overlay control plot to investigate the impact of a control parameter on the material removal rate and overcut during the machining of mild steel. Chakmakchi et al. [3] studies on the surface effects of Cu and Ti electrodes and learn more about the electrochemical characteristics of two dental alloy types

✉ Pritam Pain
pritam.me.dscsdec@gmail.com

[1] Haldia Institute of Technology, Haldia, India

[2] National Institute of Technical Teachers' Training and Research, Kolkata, India

which can be utilized in the EDM manufacture of implant-retained superstructures. The variables used in Sahuet et al.'s [4] investigation of the EDM process were peak current and pulse-on time, in conjunction with copper as the cutting tool electrode. Process responses including Surface Roughness (Ra), Material Removal Rate (MRR), White Layer Thickness (WLT) and Surface Crack Density (SCD) were assessed after tests were completed. Mohapatra and Sahoo [5] have done a comparative study of the machinability of the various types of hard alloys like Inconel 718, 825 etc. while machining by EDM process. The main objective of Sharma et al. [6] was to optimize the EDM process and also the investigation of the hybrid EDM technology by introducing nano-particles in the dielectric medium. Majumdar et al. [7] studied the effect of the presence of the graphene powder in the dielectric medium and found out that the MRR is maximum at 4% concentration of the graphene. Porwal et al. [8] have done a parametric optimization of the micro-EDM process while machining Ti alloy by using the neural network and grey relation model and developed an integrated model. Huu and Trong [9] used micro-electrode which was titanium nitride coated and it improves the surface quality of the workpiece at the optimal machining condition. Rao, T. B. [10] used metaheuristic artificial intelligence to find the predicted result of the micro-EDM process while machine Inconel 718 material. Metaheuristic texture surfaces were made by Dharmadhikari et al. [11] by employing a reverse micro EDM process. Davis et al. [12] used zinc coated micro tool made of copper and brass while machining Ti–6Al–4V alloy and made a comparison between the time of the material removal and product surface quality. The purpose of Arrabiyeh et al. [13] is to show the first-ever thorough and dependable production process for (Micropencil grinding tools) MPGTs with a cavity and to show the benefits they offer over conventional MPGTs in a machining process. Viharos and Farkas [14] developed a micro-discharge milling machine with a linear encoder, voltage, and current sensors. Utilizing the installed measuring system, the ceramic discharge milling of the $Al_2O_3$-TiC mixture was assessed. Dutta and Sarma [15] studied the effect of gap voltage, pulse on time and capacitance on the rate of material removal, rate of tool wear and overcut while machining Hastelloy C 276 by EDM process. Ekmekci et al. [16] studied a variety of pulse-on durations and pulse currents for the Ti–6Al–4V work material that was machined using SiC powder mixed with deionized water. The findings showed that the creation of secondary discharges with unequal separation boosted the rate of material transfer from the powder-mixed dielectric liquid to the machined surface through the use of the plasma channel's decomposed ions by using the Touch and Laser methods. Valentinčičet al. [17] measured the uncertainties of the volumetric and linear wear, and from the calculation, the results are shown in their publication. It was discovered that using the bigger diameter of the tool electrode and enough machining in between the two control pauses allows the touch method to assess linear wear successfully. Pandey and Anas [18] and Raju and Hiremath [19] reviewed different papers on Micro-EDM and point out the different methods of machining, different control parameters and different ways to optimize this complicated machining process. Sheelwant et al. [20] studied the machining effect on aluminum metal matrix composite material and optimized the machining variables by using an artificial neural network and then used a genetic algorithm. Roy et al. [21] used TiNiCu shape memory alloys in their research work while machining by Wire Electric Discharge Machining and optimized the control parameters by using ANN along with GA.

Micro-EDM can also be used to create precision components for spacecraft, such as propulsion systems, reaction wheels, and star trackers. Aluminum alloys and SS 204 can be used to create lightweight and durable components that meet the stringent requirements for aerospace applications. Micro-EDM can also be used to create high-precision fuel injection nozzles from aluminum and SS 204, which are used in modern gasoline and diesel engines. The process can create the small orifices and complex shapes required for these components with high accuracy and repeatability [22].

It is evident from the literature review that the four variable parameters like Voltage, Duty Factor, Frequency and Tool diameter plays a significant role while machining in Micro EDM process on the responses like Material Removal Rate and Overcut while working on Aluminum and SS204 material. The intent here is to micro EDM on two different materials where the Material removal rate and the overcut phenomenon will be observed while varying the four different control parameters like voltage (V), Duty Factor (DF), Frequency (F) along with Tool diameter (Td). Initially Analysis of Variation (ANOVA) is performed where the influence of the parameters is observed on the responses, and the effects are reflected through the interaction plot of the variables. Then the multi response optimization is done by applying Genetic algorithm. In order of converge to a single set of process parameters which will simultaneously effect both the responses, Grey Relational Analysis is performed. In order to validate the results as obtained mathematically experimentation with the given set of parameters is done and the results are compared.

## 2 Machining setup

In this research work, self-developed micro electric discharge machining (μEDM) setup has been used. Microcontroller Atmega 2560 has been used to develop the controller of this μEDM setup. Along with that various off-chip components have been used to support the microcontroller. The movement of the tool is controlled in both rotational and translational

**Table 1** Physical Properties of workpiece materials

| Category | Aluminum | SS 204 |
|---|---|---|
| Density | 2.7 g/cm$^3$ | 7.80 g/cm$^3$ |
| Hardness | 25.9HB | 201 HB |
| Modulus of Elasticity | 70 GPa | 200 GPa |
| Thermal Conductivity | 251 W/m K | 15 W/m K |
| Form | Rolled | Rolled |

directions which is unlike in the conventional micro-EDM setup. The novelty of this machining setup is that there is no tool work contact. The tool feed movement as controlled by the servo mechanism depends upon the compensation of the constant tool work gap which is almost less than one millimeter. For the translational motion, each step has been divided into four equal parts in order to attain the micro steps. Therefore there is no vibration observed during machining, unlike conventional machining processes. A program has been directly written in Arduino Integrated Development Environment (Arduino IDE). The control strategy as well as the program has been modified several times and uploaded to the controller time to time.

In this experiment, the electrode tool material for the EDM was copper (Cu). Copper is selected as an electrode due to its broad manufacturing application as well as its capacity to provide a high-quality surface finish. This tool is simple to machine and build. It can produce a mirror-like surface finish, but it is only helpful for tiny cavities where polishing is difficult [23]. Aluminum and SS-204 plates of 1 mm thickness and surface area of 50 × 25 mm$^2$ have been used as work material for experimentation. The physical properties of these materials are shown in Table 1. The chemical composition of the two different work materials is shown in Tables 2 and 3. Both these materials are ductile. One is ferrous and the other one is non-ferrous in composition. Since this is the initial stage of experimental observation for this machining setup, therefore these materials are selected. The dielectric fluid flow, DC motor, working tank with work holding device, tool holder, and servo system to feed the tool part with all components of the micro EDM setup has been shown in Fig. 1.

## 3 Planning for experimentation

It is evident that to optimize a complex process like micro-EDM, there are several parameters are involved, working voltage, pulse on time, pulse off time, Duty factor, flushing pressure of the dielectric fluid, and tool retract distance [24].

Based on the past literature review, in this research work voltage (V), Duty Factor (DF) and Frequency (F) of the spark has been considered as the control parameter along with the tool diameter (Td), while machining Aluminum and SS 204 material. The control parameters are varied in three different levels as per the L16 Orthogonal array of Taguchi design. Table 4 lists the various control parameters, along with their units and levels.

As a dielectric fluid, commercial-grade EDM-30 oil was employed, which had specific gravities of 0.80 at 25 °C and viscosity of 3.11 CSt. at 100°F (38 °C). A Micro cutting tool made of Cu with a pressure of 0.2 kgf/cm$^2$ is used for external lateral flushing. The electrode used in the experiments had a positive polarity. In different stages, the pulsed discharge current was applied in the positive mode. All other parameters like flushing pressure, type of dielectric fluid, tool retract distance etc. were kept constant during the experimentation. Here the material removal rate is the difference in the initial weight and the final weight of the workpiece material with respect to the time and measured in terms of g/s with the help of a Shimadzu (AT-R Series) Weighing Machine (Accuracy 0.001 g). Figure 2 shows the workpiece is placed on the measuring platform. The overcut is the difference between the designed hole diameter with the experimentally obtained diameter and is measured with the help of a Tool Maker's Microscope (Accuracy 3 + L/200 μm).

Since this is a micro machining process maintaining low amperage and voltage to generate the necessary decomposition potential for initiation of spark discharge is a challenge. Along with the control parameters several fixed parameter were maintained in order to have a uniform discharge potential at the electrode. Since the workpiece materials are ductile in nature therefore restricting the overcut phenomena was really challenging. Figure 3 represent the machined image of the both type workpiece materials.

**Table 2** Chemical Composition of Aluminum

| Chemical composition | Si | Fe | Cu | Mn | Mg | Zn | Ti | Al |
|---|---|---|---|---|---|---|---|---|
| Percentage | 0.2 | 0.25 | 0.04 | 0.03 | 0.03 | 0.04 | 0.03 | Balance |

**Table 3** Chemical Composition of SS204

| Chemical composition | Cr | Mn | Ni | N | Fe |
|---|---|---|---|---|---|
| Percentage | 16.00–18.00 | 6.80–8.50 | 2.00–5.00 | 0.0–0.25 | Balance |

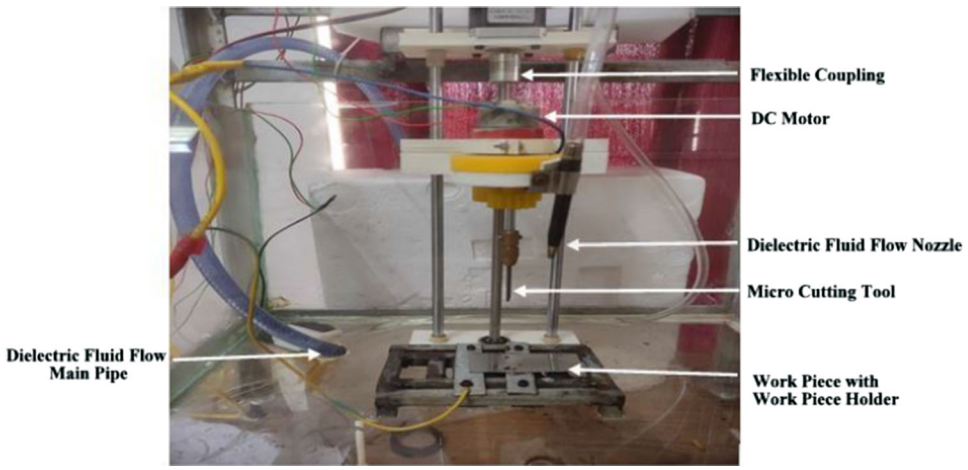


**Fig. 1** Photograph of the micro machining setup

**Table 4** Control variables along with their levels

| Control variables | Symbol | Unit | Levels | | |
|---|---|---|---|---|---|
| | | | 1st Level | 2nd Level | 3rd Level |
| Voltage | V | Volt | 30 | 40 | 50 |
| Duty Factor | DF | % | 75 | 80 | 85 |
| Frequency | F | Hz | 15 | 20 | 25 |
| Tool Diameter | Td | mm | 0.90 | 0.91 | 0.92 |

**Fig. 2** Photograph of the weighing machine along with the workpiece on it

## 4 Effect of individual control parameters on responses and their interaction plot

### 4.1 Parametric analysis for Al

#### 4.1.1 Parametric analysis for maximum MRR

Table 5 clearly shows that the F values for frequency is 22.995 and percentage contribution yield 88.46%. This suggests that the frequency has the greatest impact on the rate of material removal when cutting Aluminium as compared to the other parameters.

Figure 4 illustrates the S/N ratio graph for MRR while varying Voltage, DF, Frequency and Tool Diameter. The maximum MRR is obtained at 50 V, 85% Duty Factor, 20 Hz frequency and 0.92 mm tool diameter. It is evident from the curve that with the increase in voltage the MRR increases gradually. As the voltage increases the discharge potential increases and this lead to an increment of MRR. The duty factor is directly proportional to the MRR where with the increase in the pulse on-time more material gets removed. With the increase in frequency, the MRR increases. In the case of machining aluminum in micro EDM, increasing the current frequency can lead to an increase in MRR. This is because, at higher frequencies, the spark discharge occurs more frequently, resulting in more sparks per unit of time. This, in turn, increases the rate of material removal from the workpiece, leading to a higher MRR. When machining aluminum in micro EDM, increasing the cutting tool diameter can lead to an increase in MRR. This is because a larger cutting tool diameter leads to a larger discharge area and hence more material is removed in each spark. Additionally, a larger cutting tool diameter can also lead to a higher discharge energy, which can result in a more efficient material removal process and an increase in MRR.


**Fig. 3** Photographs of the micro drill in Aluminium and SS204 workpiece

**Table 5** ANOVA for MRR

| Source | DF | Adj SS | Adj MS | F-Value | %-Value |
|---|---|---|---|---|---|
| Voltage | 2 | 0.67738 | 0.338690 | 1.7849 | 6.87 |
| Duty Factor | 2 | 0.45706 | 0.228530 | 1.2044 | 4.63 |
| Frequency | 2 | 8.72662 | 4.363310 | 22.9950 | 88.46 |
| Tool Dia | 2 | 0.00406 | 0.002030 | 0.0107 | 0.04 |
| Error | 0 | | | | |
| Total | 8 | 9.86512 | | | |
| Pooled Error | 6 | 1.138500 | 0.189750 | 25.9950 | |

**Fig. 4** SN ratio curve for MRR of Al material

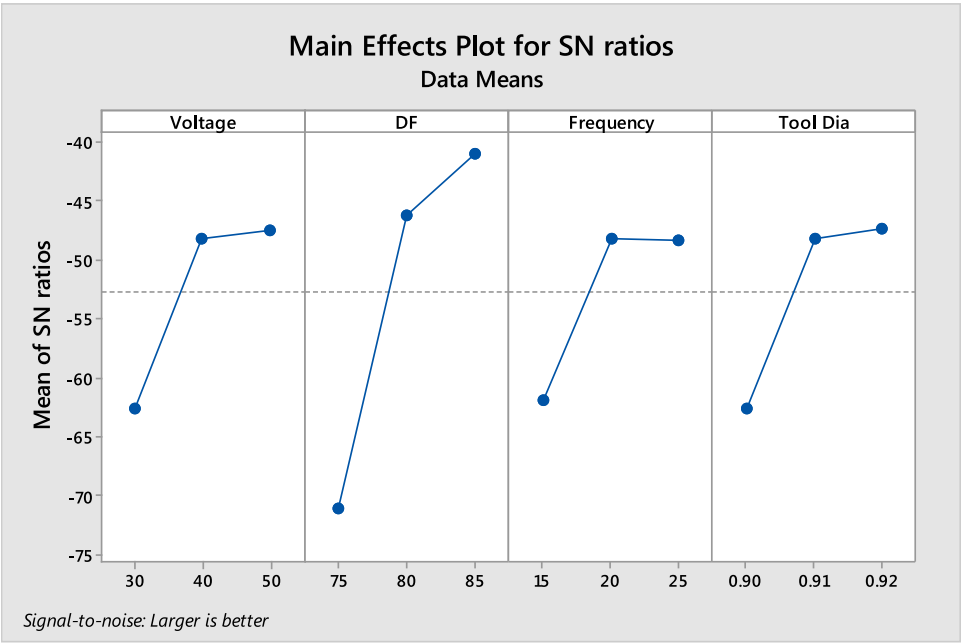

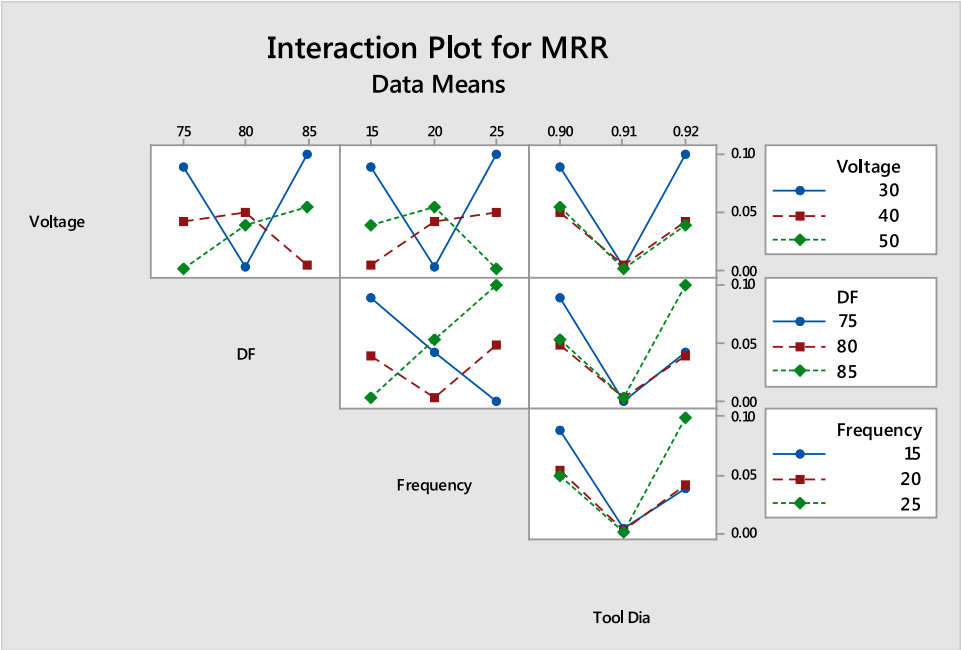


**Fig. 5** Interaction plot of control parameters for MRR of Al material

The interaction of the control parameters against the MRR while machining Al is illustrated in Fig. 5. Increasing the voltage increases the MRR up to a certain level. Beyond that level, further increases in voltage do not significantly increase the MRR. The reason for this is that higher voltages can cause excessive heat generation and thermal damage to the workpiece and tool, leading to reduced MRR and poor surface quality. The duty factor is the percentage of time that the discharge is on during each cycle. Increasing the duty factor increases the MRR up to a certain level. Beyond that level, further increases in duty factor do not significantly increase the MRR. This is because higher duty factors can lead to increased tool wear and thermal damage to the workpiece, leading to reduced MRR and poor surface quality. Increasing the frequency increases the MRR up to a certain level. Beyond that level, further increases in frequency do not significantly increase the MRR. This is because higher frequencies can cause excessive wear of the tool and reduced discharge energy, leading to reduced MRR and poor surface quality. Increasing the tool diameter increases the MRR up to a certain level. Beyond that level, further increases in tool diameter do not significantly increase the MRR. This is because larger tool diameters require higher discharge energies, which can lead to reduced discharge efficiency and lower MRR.

### 4.1.2 Parametric analysis for maximum OC

Table 6 clearly shows that the F values for duty factor has the value of 3.2053 and an expected yield of 51%. This suggests that the duty factor has the greatest impact on the overcut followed by tool diameter when machining Aluminium.

The minimum OC is obtained at 30 V, 75% Duty Factor, 15 Hz frequency and 0.90 mm tool diameter. The increase in voltage in the micro EDM process can lead to an increase in the overcut, especially when machining aluminum (Al) materials. This is because when the voltage is increased; the electrical discharge energy between the electrode and the workpiece also increases, leading to a more intense discharge and higher temperatures at the point of contact.

At high discharge energies, the aluminum material can undergo thermal expansion, leading to the formation of a molten layer around the discharge point. This molten layer can act as a heat sink, reducing the energy available for the discharge and causing the discharge to spread out, resulting in an overcut. When the duty factor is increased, the pulse-on time is also increased, which leads to a longer duration of spark discharge and higher plasma channel temperature. This higher temperature results in more melting and vaporization of the aluminum material, which increases the overcut. Additionally, the longer duration of spark discharge can lead to the formation of a larger heat-affected zone, which can further contribute to the overcut. With the increase in frequency, the overcut varies insignificantly. From Fig. 6 it has been observed that the overcut increases with the increase in tool diameter.

The reason for the increase in overcut with the increase in tool diameter in micro EDM of aluminum is due to the distribution of electric current during the spark discharge. During the EDM process, a high-intensity electric pulse is applied to the tool or electrode, which generates a plasma

**Table 6** ANOVA for OC

| Source | DoF | Adj SS | Adj MS | F-Value | %-Value |
|---|---|---|---|---|---|
| Voltage | 2 | 0.04326 | 0.021630 | 0.2568 | 4.14 |
| Duty Factor | 2 | 0.54 | 0.270000 | 3.2053 | 51.65 |
| Frequency | 2 | 0.00011 | 0.000055 | 0.0007 | 0.01 |
| Tool Dia | 2 | 0.46204 | 0.231020 | 2.7426 | 44.20 |
| Error | 0 | | | | |
| Total | 8 | 1.04541 | | | |
| Pooled Error | 6 | 0.505410 | 0.084235 | 6.2053 | |

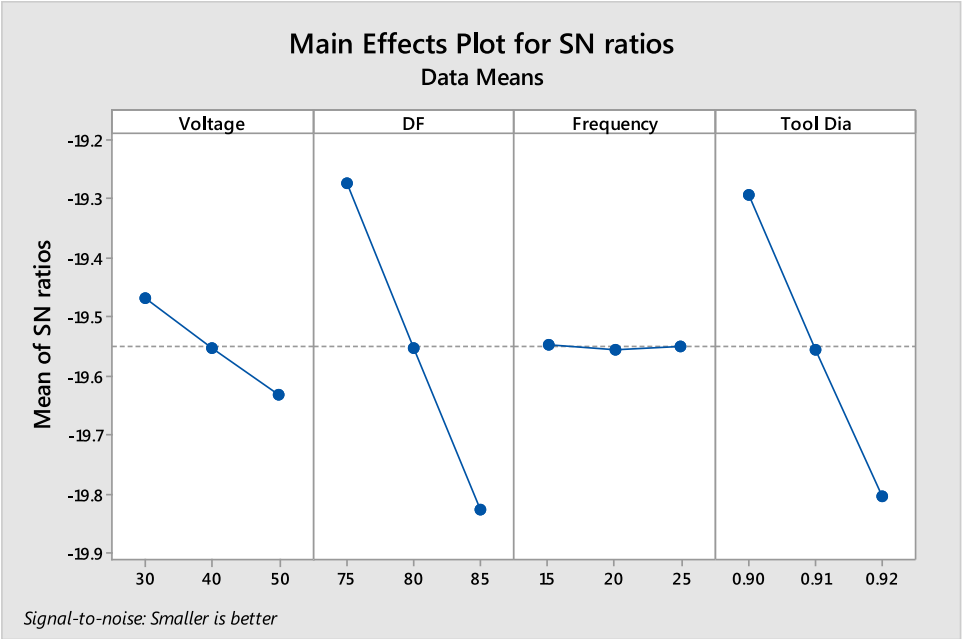


**Fig. 6** SN ratio curve for OC of Al material

channel between the tool and the workpiece. This plasma channel has a high temperature and pressure, which can cause melting and vaporization of the aluminum material, resulting in the desired cut.

The interaction of the control parameters against the OC while machining Al is illustrated in Fig. 7. The voltage controls the energy input to the machining process. A higher voltage results in higher energy input, which leads to a larger spark and deeper penetration of the tool into the workpiece. However, a higher voltage also increases the overcut. The effect of voltage on overcut is more pronounced for smaller tool diameters. Therefore, for smaller tool diameters, a lower voltage should be used to minimize the overcut. A higher duty factor results in longer discharge pulses, which leads to deeper penetration of the tool into the workpiece. However, a higher duty factor also increases the overcut. The effect of the duty factor on overcut is more pronounced for larger tool diameters. Therefore, for larger tool diameters, a lower duty factor should be used to minimize the overcut. The frequency controls the number of discharge pulses per unit of time. A higher frequency results in a larger number of discharge pulses, which can lead to a reduction in the overcut. However, a very high frequency can also cause sparking instability, which can increase in overcut. The effect of frequency on overcut is less pronounced for larger tool diameters. Therefore, a higher frequency can be used for larger tool diameters to reduce the overcut. The tool diameter affects the machining depth and the size of the spark. Smaller tool diameters result in shallower penetration and smaller sparks, which can lead to a smaller overcut. However, smaller tool diameters also result in a higher sensitivity to the control parameters. Therefore, the control parameters must be carefully optimized for smaller tool diameters to minimize the overcut.

In summary, to minimize the overcut in micro EDM on aluminum, the control parameters must be carefully optimized for the tool diameter. For smaller tool diameters, a lower voltage and duty factor should be used, while for larger tool diameters, a higher frequency can be used. Additionally, the tool diameter must be carefully selected to balance the

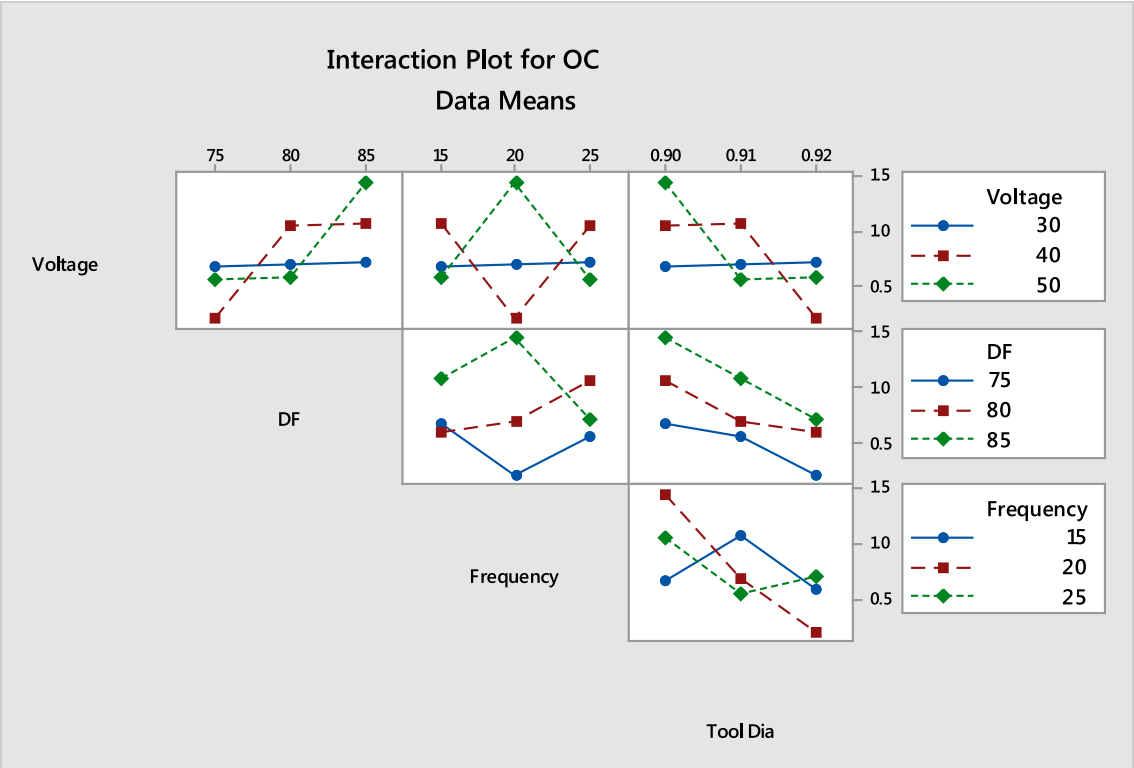


**Fig. 7** Interaction plot of control parameters for OC of Al material

desired machining depth and the sensitivity to the control parameters.

## 4.2 Parametric analysis for SS 204

### 4.2.1 Parametric analysis for maximum MRR

It is evident from Table 7 that the F-Value for frequency has the highest value 22.995 for frequency in the case of material removal of SS 204 material. It has a percentage contribution of 88.46%.

The maximum MRR is obtained at 50 V, 85% Duty Factor, 15 Hz frequency, and 0.91 mm tool diameter. From Fig. 8 it is evident that with the increase in voltage, the MRR increases steadily. As the voltage increases, the electrical energy per discharge also increases. This increased energy can cause more material to be removed during each discharge, leading to a higher MRR. As the duty factor increases the MRR gradually increases. This is because when the duty factor is increased, the energy input during the pulse-on time also increases. This causes an increase in the temperature of the workpiece material, leading to higher melting and vaporization rates, and ultimately resulting in higher MRR. With the increase in current frequency, the MRR decreases. When the current frequency is increased beyond a certain point, the MRR in the micro EDM process decreases when machining SS204. This is because, at high current frequencies, the discharge energy is distributed over shorter periods, resulting in less time for the discharge to create a plasma channel between the electrode and the workpiece. As a result, the discharge energy is not effectively utilized for material removal, leading to a decrease in MRR. The effect of tool diameter has a very nominal effect on MRR.

In this plot as illustrated in Fig. 9, voltage and duty factor are varied on the x and y-axis, respectively, while the frequency is held constant at 15 kHz and the tool diameter is held constant at 0.9 mm. The panels represent the MRR values for different combinations of frequency and tool diameter. The lines connecting the points on the plot show the interaction effect between voltage and duty factor on the MRR, while holding the other two parameters constant. This interaction plot can help us to identify the optimal combination of control parameters that maximizes the MRR for the micro-EDM process of SS 204 material.

### 4.2.2 Parametric analysis for minimize OC

It is observed from the ANOVA Table 8 that the F-value and % contribution of voltage has the value 2.6947 and 47.32 respectively which is a significant parameter as compared to the others. The minimum OC is obtained at 30 V, 75% Duty Factor, 15 Hz frequency, and 0.90 mm tool diameter as shown

**Table 7** ANOVA for MRR

| Source | DoF | Adj SS | Adj MS | F-Value | %-Value |
|---|---|---|---|---|---|
| Voltage | 2 | 0.67738 | 0.338690 | 1.7849 | 6.87 |
| Duty Factor | 2 | 0.45706 | 0.228530 | 1.2044 | 4.63 |
| Frequency | 2 | 8.72662 | 4.363310 | 22.9950 | 88.46 |
| Tool Dia | 2 | 0.00406 | 0.002030 | 0.0107 | 0.04 |
| Error | 0 | | | | |
| Total | 8 | 9.86512 | | | |
| Pooled Error | 6 | 1.138500 | 0.189750 | 25.9950 | |

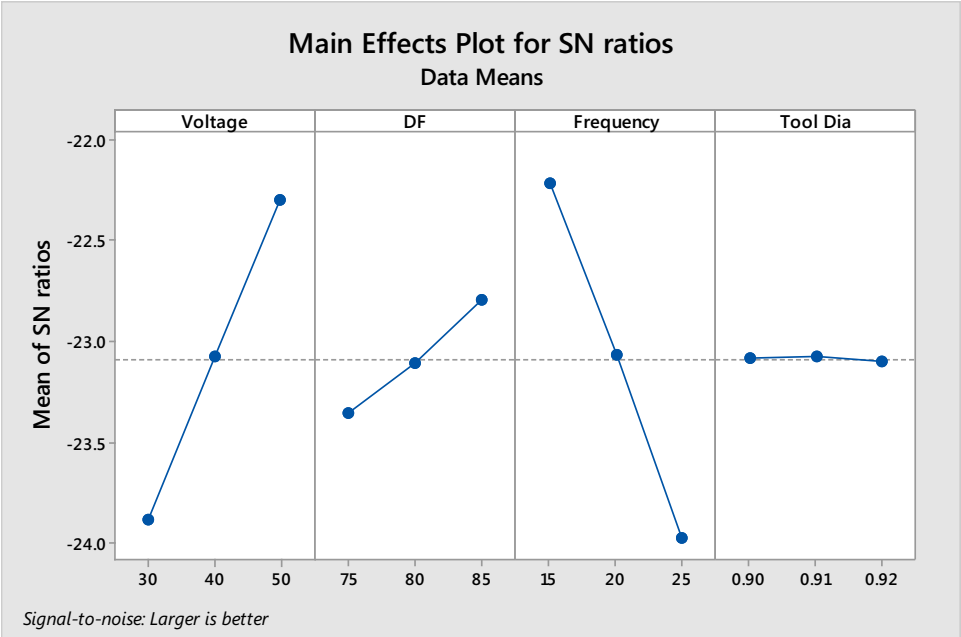


**Fig. 8** SN ratio curve for MRR of SS 204 material

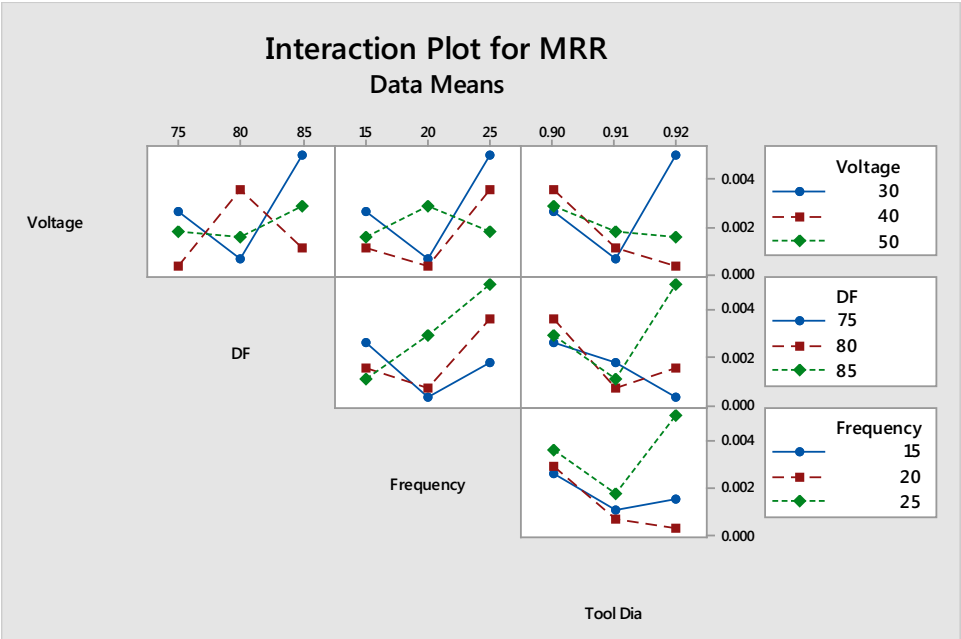


**Fig. 9** Interaction plot of control parameters for MRR of SS 204 material

**Table 8** ANOVA for OC

| Source | DF | Adj SS | Adj MS | F-Value | %-Value |
|---|---|---|---|---|---|
| Voltage | 2 | 0.31947 | 0.159735 | 2.6947 | 47.32 |
| Duty Factor | 2 | 0.03678 | 0.018390 | 0.3102 | 5.45 |
| Frequency | 2 | 0.23567 | 0.117835 | 1.9878 | 34.91 |
| Tool Dia | 2 | 0.08322 | 0.041610 | 0.7019 | 12.33 |
| Error | 0 | | | | |
| Total | 8 | 0.67514 | | | |
| Pooled Error | 6 | 0.355670 | 0.059278 | 5.6947 | |

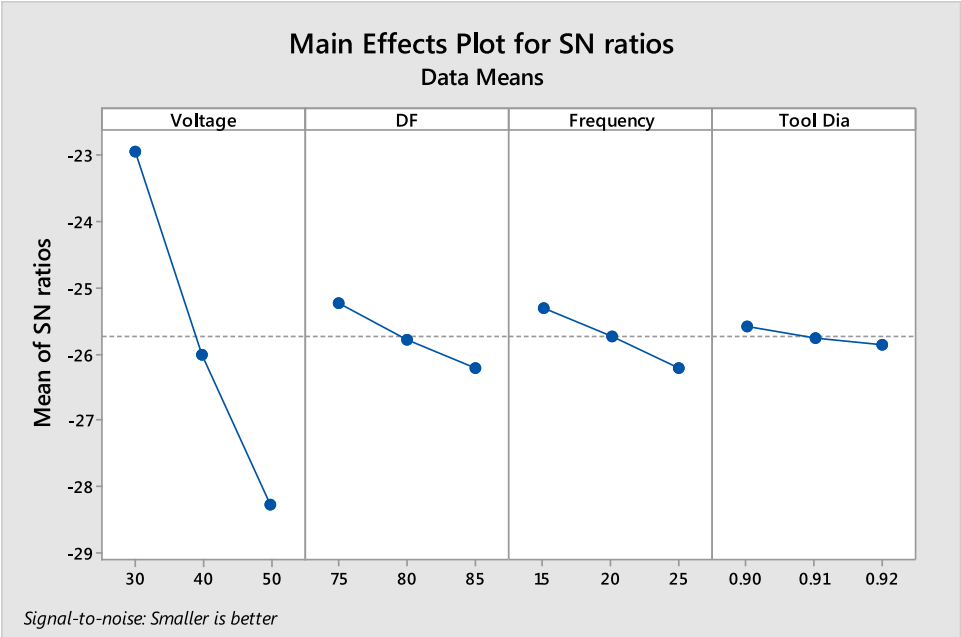


**Fig. 10** SN ratio curve for OC of SS 204 material

in Fig. 10. With the increase in voltage, the OC increases. Here increasing the voltage can lead to an increase in the electrical discharge energy, which can cause more material to be eroded from the workpiece. This can increase the overcut. With the increase in duty factor, the MRR increases. Here an increase in duty cycle is mainly due to the increase in energy delivered to the workpiece, which causes more material to be removed from the workpiece beyond the intended shape or size. With the increase in current frequency, the Overcut increases. Here an increase in frequency can lead to increased overcut due to the combination of material properties and the behavior of the electrical discharge at higher frequencies. With the increase in tool diameter, the Overcut increases. This is because a larger tool diameter leads to a larger discharge gap between the tool and the workpiece, which results in a larger volume of material being removed during each electrical discharge.

The interaction plot in Fig. 11 shows how the response variable (in this case, the output of the micro EDM process for SS 204 material) changes with changes in two or more control parameters while holding all other parameters constant. The control parameters in question are voltage, duty factor, current frequency, and tool diameter.

The effect of the interaction plot of these control parameters can be analyzed as follows:

Higher voltage generally leads to a higher discharge energy and a larger discharge crater, which can increase the overcut. Higher duty factor, on the other hand, leads to a longer duration of the discharge and a larger total amount of material removed, which can also increase the overcut. Higher frequency, on the other hand, leads to a shorter discharge duration and a smaller discharge crater, which can decrease the overcut.

The specific combination of voltage and frequency that leads to the lowest overcut will depend on the specific experimental conditions, such as the electrode material, the workpiece material, the gap distance, and the machining time.

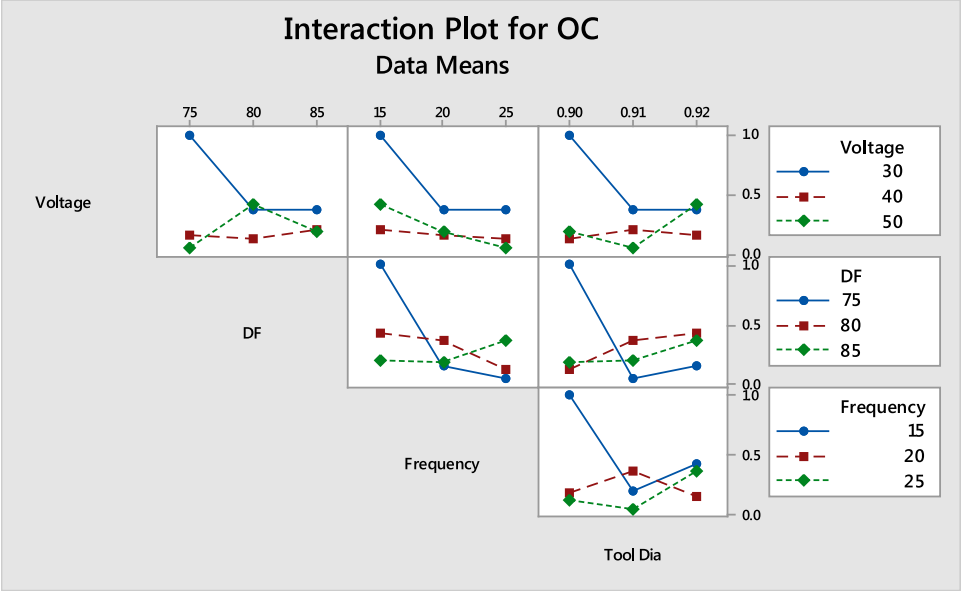


**Fig. 11** Interaction plot of control parameters for OC of SS 204 material

In general, a lower voltage and a smaller tool diameter will lead to lower overcut, but this may also result in a slower material removal rate and longer machining time.

## 5 Multi-objective genetic algorithm (M-GA)

M-GA is a metaheuristic optimization algorithm that is based on the principles of evolution and natural selection. It follows these basic steps.

It creates an initial population of solutions randomly. Then evaluate the fitness of each solution in the population according to the multiple objectives that need to be optimized. After that, it selects the best solutions from the population based on their fitness. Then it generates new solutions by using crossover and mutation operators on the selected solutions. Finally, it evaluates the fitness of the new solutions. Then it replaces the worst solutions in the population with new solutions. The mathematical equation for a MOGA can be written as follows:

$$\min\ f(x) = [f1(x), f2(x), \ldots,\ fm(x)] \tag{1}$$

subject to: $gi(x) < = 0$, $i = 1,2,\ldots,k$where x is the solution vector, f(x) is the vector of objective functions, gi(x) are the constraints, and k is the number of constraints [25].

### 5.1 Result analysis using the genetic algorithm

Finding a single parametric combination for these diametrically opposed parameters was the aim of employing multi-response optimization [26]. Figuring out the two opposing criteria, such a high rate of material remove and a low OVERCUT. A genetic algorithm's boundary condition is as follows:

- Double vector type of population
- Stopping Criteria is
  - While the generation is greater than the 100 times of the number of the variables
  - While the generation of Stall cross 100
  - When the function tolerance falls below to $1 \times 10^{-4}$
  - When the constrain tolerance falls below to $1 \times 10^{-3}$
  - There is no time constrain

Due to the competing nature of the objectives, multi-response optimization is used to accomplish the goal with just one set of parameters. Due to the complexity of the EDM machining process, there are two common uses for it in industry. In one instance, maximizing MRR is the main goal. It is suitable for crude cutting. In a different scenario, overcut should be prioritized over MRR for the completing procedure. In this circumstance, tool wear has a significant impact on the product's final geometry. Since the genetic algorithm is typically used for minimalize functions, the negative (-ve) sign has been disregarded in the instance of maximizing MRR [27] (Table 8).

#### 5.1.1 Result analysis of Al data by using M-GA

At this time, the overall count of optimization calculations needed is 127, which results in 13 blends of the variables and objectives. Once the mean variation in the range of Pareto solutions touched the tolerance cost, optimization was ended.

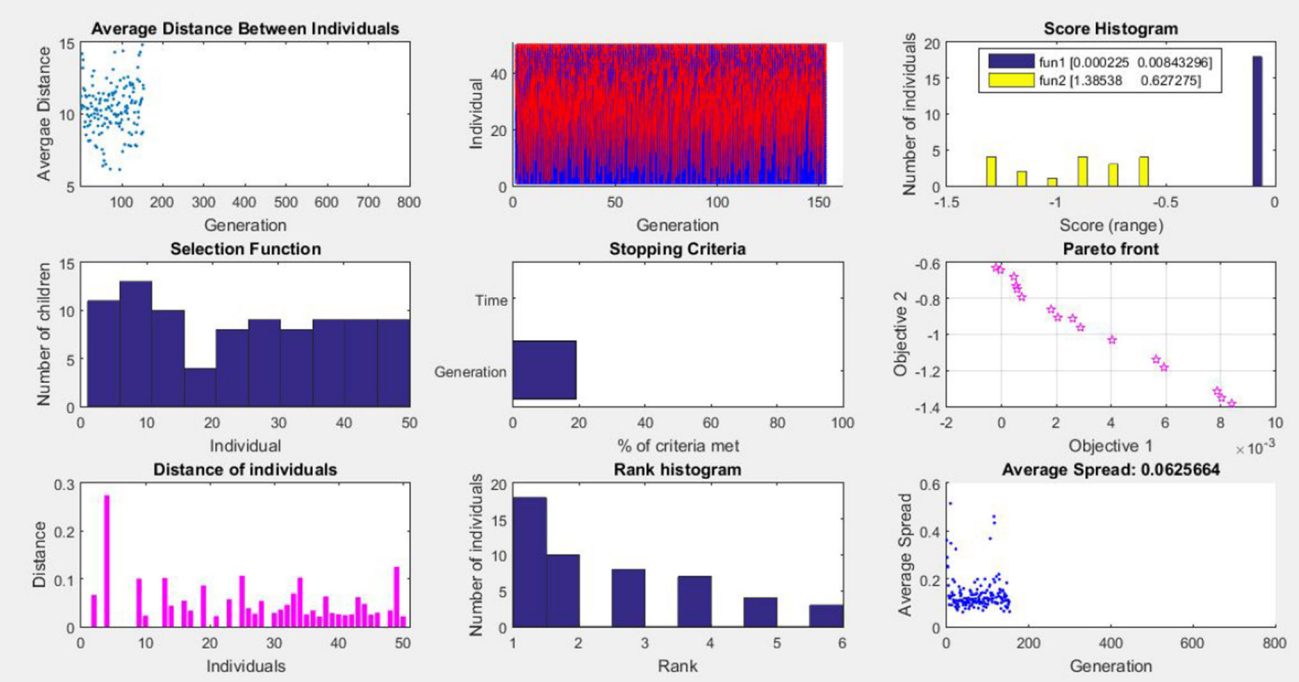


**Fig. 12** Plot functions of GA for Al

**Table 9** Combination of factors and responses for Al

| Sl. no. | Voltage (v) | DF (%) | Frequency (Hz) | Tool Dia (mm) | MRR (g/s) | OC (mm) |
|---|---|---|---|---|---|---|
| 1 | 43 | 75 | 16 | 0.90 | 0.001 | 0.79 |
| 2 | 49 | 84 | 18 | 0.90 | 0.008 | 1.39 |
| 3 | 48 | 78 | 16 | 0.90 | 0.003 | 0.96 |
| 4 | 49 | 76 | 16 | 0.90 | 0.002 | 0.91 |
| 5 | 47 | 84 | 18 | 0.90 | 0.008 | 1.31 |
| 6 | 44 | 79 | 17 | 0.90 | 0.004 | 1.03 |
| 7 | 45 | 77 | 17 | 0.90 | 0.003 | 0.91 |
| 8 | 37 | 75 | 15 | 0.90 | 0.001 | 0.73 |
| 9 | 38 | 75 | 16 | 0.90 | 0.001 | 0.75 |
| 10 | 42 | 76 | 16 | 0.90 | 0.002 | 0.86 |
| 11 | 44 | 82 | 17 | 0.90 | 0.006 | 1.18 |
| 12 | 44 | 81 | 17 | 0.90 | 0.006 | 1.14 |
| 13 | 49 | 84 | 18 | 0.90 | 0.008 | 1.35 |

The two opposing objectives that are simultaneously maximized via GA are shown in Fig. 12. The boundary conditions for MRR and OC can be deduced from this plot. The range for MRR is 0.001–0.005 g/s, while for OC, it ranges from 0.73 to 1.39 mm. Pareto front plot shows the trade-off between MRR and overcut. The x-axis represents MRR and the y-axis represents overcut. The Pareto front in Fig. 12 shows as a set of non-dominated points, and here it is converging in nature. The rank is calculated by assigning a score to each parameter based on how much it contributes to the objective function. From there histogram plot shows the distribution of the process parameters that lead to the optimal solutions on the Pareto front.

As this optimization technique generates a set of parametric combinations, therefore Fuzzy Gray Relational Analysis is used to find an ideal or nearly ideal combinations of variable that will successively gratify the contradicting character of the objectives.

Table 9 displays the various parametric combinations and corresponding responses as determined by GA.

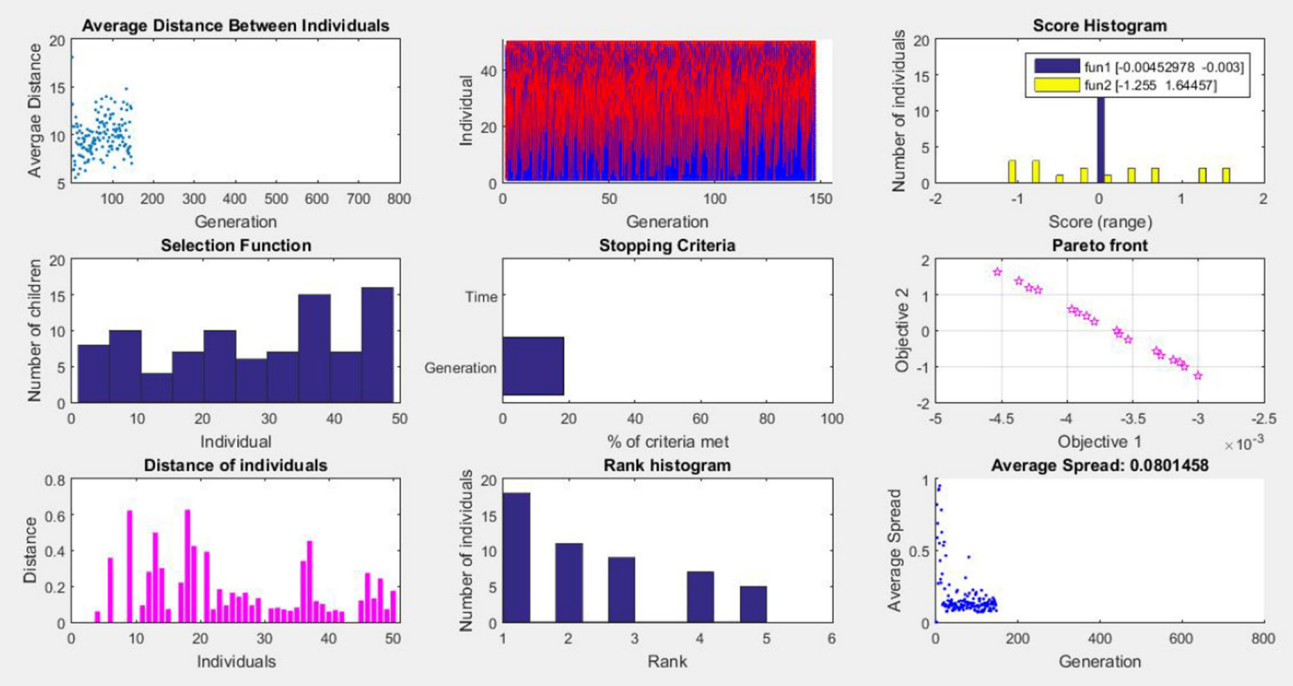


**Fig. 13** Plot functions of GA for SS-204

#### 5.1.2 Result analysis of SS 204 data by using M-GA

At this time, the overall count of optimization calculations needed is 148, that results in 16 combinations of the control parameters and replies. Once the mean variation in the range of Pareto solutions touched the tolerance cost, optimization was ended. The two opposing objectives that are simultaneously maximized via GA are shown in Fig. 13. The boundary conditions for MRR and OC can be deduced from this plot. The range for MRR is 0.003–0.005 g/s, while for OC, it ranges from 0.01 to 1.64 mm. A Pareto front shows the tradeoff between two objectives in the Fig. 13. In the context of SS204, material removal rate can be plotted on the x-axis and overcut on the y-axis. Each point on the Pareto front represents a solution that is not dominated by any other solution. The Pareto front helps us visualize the tradeoff between material removal rate and overcut and identify the optimal solutions. This rank plot shows the fitness (objective function value) of the best solution found by the GA in each generation. A histogram shows the distribution of the objective function values for all the solutions in the population. This plot helps us see how the solutions are distributed and identify if there are any patterns or clusters.

Fuzzy Gray Relational Analysis is therefore used to find an ideal or nearly ideal combination of variable that will successively gratify the contradicting character of the objectives.

Table 10 displays the various parametric combinations and corresponding responses as determined by GA.

## 6 Analysis of multi-criteria decision making (MCDM)

The dual contradicting responses, MRR and OC, have different levels of rank in this study [28]. Instead of the decreased OC, the maximal MRR is the main goal in this situation.

The state where the largest importance is required, such as MRR, has a normalized equation that is represented as:

$$X_{ij} = \frac{Y_{ij} - Min\left[Y_{ij},\, i = 1, 2, \ldots n\right]}{Max\left[Y_{ij},\, i = 1, 2, \ldots n\right] - Min\left[Y_{ij},\, i = 1, 2, \ldots n\right]} \tag{2}$$

In the case of overcut, a lower value for greater performance is stated as,

$$X_{ij} = \frac{Max\left[Y_{ij},\, i = 1, 2, \ldots n\right] - Y_{ij}}{Max\left[Y_{ij},\, i = 1, 2, \ldots n\right] - Min\left[Y_{ij},\, i = 1, 2, \ldots n\right]} \tag{3}$$

From GA a pool of global optimal solutions are predicted. Therefore we need to converge to a specific set of parametric combination will be satisfy the contradictory responses. Then Grey Relational Analysis (GRA) is used to determine the pool of global optima to a single set of process parameters that will simultaneously comply with the responses.

**Table 10** Combination of factors and responses for SS-204

| Sl. no. | Voltage (V) | DF (%) | Frequency (Hz) | Tool Dia (mm) | MRR (g/s) | OC (mm) |
|---|---|---|---|---|---|---|
| 1 | 56 | 70 | 15 | 0.9 | 0.005 | 1.64 |
| 2 | 34 | 70 | 15 | 0.9 | 0.003 | 0.83 |
| 3 | 40 | 70 | 15 | 0.9 | 0.004 | 0.11 |
| 4 | 46 | 70 | 15 | 0.9 | 0.004 | 0.50 |
| 5 | 43 | 70 | 15 | 0.9 | 0.004 | 0.25 |
| 6 | 45 | 70 | 15 | 0.9 | 0.004 | 0.40 |
| 7 | 52 | 70 | 15 | 0.9 | 0.004 | 1.19 |
| 8 | 30 | 70 | 15 | 0.9 | 0.003 | 1.25 |
| 9 | 54 | 70 | 15 | 0.9 | 0.004 | 1.37 |
| 10 | 47 | 70 | 15 | 0.9 | 0.004 | 0.59 |
| 11 | 32 | 70 | 15 | 0.9 | 0.003 | 1.02 |
| 12 | 39 | 70 | 15 | 0.9 | 0.004 | 0.24 |
| 13 | 51 | 70 | 15 | 0.9 | 0.004 | 1.12 |
| 14 | 41 | 70 | 15 | 0.9 | 0.004 | 0.01 |
| 15 | 36 | 70 | 15 | 0.9 | 0.003 | 0.56 |
| 16 | 35 | 70 | 15 | 0.9 | 0.003 | 0.70 |

**Table 11** Fuzzy weight calculation

| Linguistic terms | Fuzzy number | | | qi |
|---|---|---|---|---|
| MRR- Very High | 0.9 | 1 | 1 | 0.84375 |
| OC-Moderately Low | 0.1 | 0.3 | 0.5 | 0.15625 |

**Table 12** Grades and rankings for Al, together with the grey connection coefficient

| Exp no. | Control parameter | | | | Response | | GREY grade | Rank |
|---|---|---|---|---|---|---|---|---|
| | Voltage (V) | Duty factor (%) | Frequency (Hz) | Tool Dia (mm) | MRR (g/s) | OC (mm) | | |
| 1 | 43 | 75 | 16 | 0.90 | 0.001 | 0.79 | 0.584 | 6 |
| 2 | **49** | **84** | **18** | **0.90** | **0.008** | **1.39** | **0.680** | **1** |
| 3 | 48 | 78 | 16 | 0.90 | 0.003 | 0.96 | 0.497 | 12 |
| 4 | 49 | 76 | 16 | 0.90 | 0.002 | 0.91 | 0.514 | 11 |
| 5 | 47 | 84 | 18 | 0.90 | 0.008 | 1.31 | 0.624 | 5 |
| 6 | 44 | 79 | 17 | 0.90 | 0.004 | 1.03 | 0.494 | 13 |
| 7 | 45 | 77 | 17 | 0.90 | 0.003 | 0.91 | 0.521 | 8 |
| 8 | 37 | 75 | 15 | 0.90 | 0.001 | 0.73 | 0.652 | 2 |
| 9 | 38 | 75 | 16 | 0.90 | 0.001 | 0.75 | 0.630 | 4 |
| 10 | 42 | 76 | 16 | 0.90 | 0.002 | 0.86 | 0.541 | 7 |
| 11 | 44 | 82 | 17 | 0.90 | 0.006 | 1.18 | 0.515 | 9 |
| 12 | 44 | 81 | 17 | 0.90 | 0.006 | 1.14 | 0.515 | 10 |
| 13 | 49 | 84 | 18 | 0.90 | 0.008 | 1.35 | 0.633 | 3 |

The GRA is used to determine the single solution to these two opposing processes. The best answer amongst the comparison sequences is provided by the closed value to 1 [29, 30]. In this instance, 13 and 16 simulated data for Al and SS 204, respectively, from the genetic method have been used for further evaluation. The maximum MRR and the minimal OC have been established as the decision-making criteria in this scenario.

According to calculations made using fuzzy set theory in the Table 11, the specified weights for MRR and OC are

**Table 13** Along with grades and rankings, the grey relation coefficient for the SS 204

| Exp no. | Control parameter | | | | Response | | GREY grade | Rank |
|---|---|---|---|---|---|---|---|---|
| | Voltage (V) | Duty factor (%) | Frequency (Hz) | Tool Dia (mm) | MRR (g/s) | OC (mm) | | |
| 1 | 56 | 70 | 15 | 0.9 | 0.005 | 1.64 | 0.680 | 3 |
| 2 | 34 | 70 | 15 | 0.9 | 0.003 | 0.83 | 0.416 | 14 |
| 3 | 40 | 70 | 15 | 0.9 | 0.004 | 0.11 | 0.684 | 2 |
| 4 | 46 | 70 | 15 | 0.9 | 0.004 | 0.5 | 0.559 | 7 |
| 5 | 43 | 70 | 15 | 0.9 | 0.004 | 0.25 | 0.629 | 5 |
| 6 | 45 | 70 | 15 | 0.9 | 0.004 | 0.4 | 0.584 | 6 |
| 7 | 52 | 70 | 15 | 0.9 | 0.004 | 1.19 | 0.452 | 11 |
| 8 | 30 | 70 | 15 | 0.9 | 0.003 | 1.25 | 0.365 | 16 |
| 9 | 54 | 70 | 15 | 0.9 | 0.004 | 1.37 | 0.435 | 13 |
| 10 | 47 | 70 | 15 | 0.9 | 0.004 | 0.59 | 0.539 | 8 |
| 11 | 32 | 70 | 15 | 0.9 | 0.003 | 1.02 | 0.390 | 15 |
| 12 | 39 | 70 | 15 | 0.9 | 0.004 | 0.24 | 0.633 | 4 |
| 13 | 51 | 70 | 15 | 0.9 | 0.004 | 1.12 | 0.459 | 10 |
| 14 | **41** | **70** | **15** | **0.9** | **0.004** | **0.01** | **0.733** | **1** |
| 15 | 36 | 70 | 15 | 0.9 | 0.003 | 0.56 | 0.465 | 9 |
| 16 | 35 | 70 | 15 | 0.9 | 0.003 | 0.7 | 0.437 | 12 |

**Table 14** Comparison study of single objective functions

| Materials | Responses | Parametric combination | | | | Predicted results |
|---|---|---|---|---|---|---|
| | | Voltage (V) | Duty Factor (%) | Frequency (Hz) | Tool Dia (mm) | |
| AL | MRR (g/s) | 50 | 85 | 20 | 0.92 | 0.008 |
| | OC (mm) | 30 | 75 | 15 | 0.90 | 0.884 |
| SS 204 | MRR (g/s) | 50 | 85 | 15 | 0.91 | 0.086 |
| | OC (mm) | 30 | 75 | 15 | 0.90 | 0.123 |

84.4% and 15.6%, respectively, in both Al and SS 204 materials.

## 6.1 Optimization of the parameters for aluminum

For the Al material in Table 2, Table 12 shows the grey relation coefficient and rank corresponding to the parametric parameters and responses.

Table 12 shows the ranks, relation grade, and grey relation coefficient. It is clear from this table that experimental run number 2 has attained the highest grey relation grade (indicated in Bold). This experimental run satisfies the need for the optimized multi-response parameter, as was previously discussed. The greatest results were obtained in experiment 2, which used a 49 V voltage difference between the tool and the workpiece, an 84% duty factor (DF), and an 18 Hz frequency and 0.9 mm tool diameter as input parameters. This experiment had a high MRR and a low Overcut.

## 6.2 Optimization of the parameters for Stainless Steel (SS 204)

By parametric settings and responses, Table 13 shows the grades and the grey relation coefficient for the material in Table 3.

Table 13 shows the ranks, relation grade, and grey relation coefficient. It is clear from this table that experimental run number 14 has attained the highest grey relation grade (indicated in Bold). As was previously said, this experimental run satisfies the requirement for the optimized multi-response parameter. Therefore, experiment 14 produced the best results, with high MRR and minimal Overcut. It used a 41 V voltage difference between the tool and the workpiece, a 70% duty factor (DF), and a 15 Hz frequency and 0.9 mm tool diameter as input parameters.

**Table 15** Comparison study of multi-objective functions

| Material | Control parameter | | | | Predicted response | | Validation result | | | | Improv-ement of Grey Grade |
|---|---|---|---|---|---|---|---|---|---|---|---|
| | Volt-age (V) | DF (%) | Frequ-ency (Hz) | Tool Dia (mm) | MRR (g/s) | OC (mm) | Initial Wt. (g) | Final Wt. (g) | Final MRR (g/s) | OC (mm) | |
| Al | 49 | 84 | 18 | 0.9 | 0.008 | 1.39 | 1.092 | 1.084 | 0.008 | 1.37 | 0.05 |
| SS 204 | 41 | 70 | 15 | 0.9 | 0.004 | 0.010 | 6.434 | 6.430 | 0.004 | 0.008 | 0.01 |

## 7 Comparison study

Comparison of single objective optimization of individual parameters one at a time for Al and SS are shown in Table 14.

The parametric combination for two contradictory objective MRR and OC for Al and SS 204 has been shown in Table 15.

Here the validation experimentation concerning MRR and OC while machining Al and SS 204 is performed while considering the control parameters. It has been observed that there is an improvement in response values which indicates that the experimentation has been validated successfully. Figure 14 represent the microscopic view of the validated test on both materials namely Aluminum and SS204.

## 8 Conclusion

The parametric analysis and optimization by using a micro EDM setup while machining Aluminum and SS204 have been successfully conducted. The following inferences can be made:

1. Initially, ANOVA is performed to estimate the effect of the controlled parameters on the responses and their subsequent interaction while machining these materials.
2. The results from ANOVA show that Frequency is the main influencing parameter of MRR while machining Aluminium and Duty Factor is the significant process parameter in case of Overcut. Similarly Frequency is the most influencing parameter for MRR while machining SS204 and Voltage is the significant process parameter for Overcut.
3. It has been observed from the S/N ratio plots, that the maximum MRR is obtained at 50 V, 85% Duty Factor, 20 Hz frequency, and 0.92 mm tool diameter while machining Al material.
4. Subsequently, the minimum OC has been observed at 30 V, 75% Duty Factor, 15 Hz frequency, and 0.90 mm tool diameter for the same material.
5. The maximum MRR is obtained at 50 V, 85% Duty Factor, 15 Hz frequency, and 0.91 mm tool diameter while machining SS204.
6. The minimum OC is obtained at 30 V, 75% Duty Factor, 15 Hz frequency, and 0.90 mm tool diameter while machining SS204.
7. In case of multi-objective optimization while machining Aluminum, to achieve high MRR and low Overcut the input parameters to be considered are 49 Volt voltage, 84% duty factor (DF), 18 Hz frequency with 0.9 mm tool diameter. Similarly following the multi-objective optimization technique while machining SS204 against the

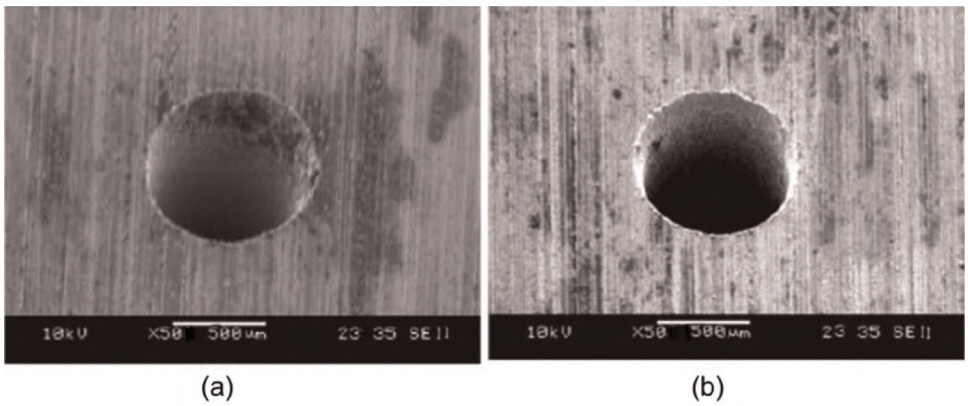


**Fig. 14** Microscopic view of the validation test **a** Aluminum, **b** SS204 material

same set of the condition of high MRR and low Overcut the single set of control parameters to be considered are 41 V voltage, 70% duty factor (DF), 15 Hz frequency, and 0.90 mm tool diameter.

8. While comparing the two multi-objective results of the two work materials viz. Aluminum and SS204, confirmation tests were conducted with the same set of parameters as obtained analytically. There has been an indication of improvement in the experimental results.

Hence these parametric combinations can act as a guideline for researchers and industry personnel who are working with micro EDM while machining Aluminum and SS204 materials. These two materials have an as wide range of applications in the aerospace and automotive industries. Therefore precision machining of these materials is a challenge. Therefore the exact control parameter values which are predicted through this research work will provide the impetus for machining these materials commercially.

## References


1. Gholipoor, A., Baseri, H., Shabgard, M.R.: Investigation of near dry EDM compared with wet and dry EDM processes. J. Mech. Sci. Technol. **29**, 2213–2218 (2015)
2. Bose, G.K., Pain, P.: Metaheuristic approach of multi-objective optimization during EDM process. Int. J. Math. Eng. Manag. Sci. **3**, 301–314 (2018)
3. Chakmakchi, M., Ntasi, A., Mueller, W.D., Zinelis, S.: Effect of Cu and Ti electrodes on surface and electrochemical properties of Electro Discharge Machined (EDMed) structures made of Co-Cr and Ti dental alloys. Dent. Mater. **37**, 588–596 (2021)
4. Sahu, S.K., Jadam, T., Datta, S.: Study of machinability assessment of nickel based alloy using electro-discharge machining with transformer oil as dielectric. Mater. Today Proc. **38**, 2205–2212 (2021)
5. Mohapatra, S., Sahoo, A.K.: Comparative study of inconel 601, 625, 718, 825 super-alloys during electro-discharge machining. Mater. Today Proc. **56**, 226–230 (2022)
6. Sharma, P., Kishore, K., Sinha, M.K., Singh, V.: Electrical discharge machining of nickel-based superalloys: a comprehensive review. Int. J. Mater. Eng. Innov. **13**, 157 (2022)
7. Majumdar, S., Bhoi, N.K., Singh, H.: Graphene nano-powder mixed electric discharge machining of Inconel 625 alloy: optimization of process parameters for material removal rate. Int. J. Interact. Design Manuf. (IJIDeM), 2022
8. Porwal, R.K., Yadava, V., Ramkumar, J.: Modelling and multi-response optimization of hole sinking electrical discharge micro-machining of titanium alloy thin sheet. J. Mech. Sci. Technol. **28**, 653–661 (2014)
9. Huu, P.N., Trong, L.N.: Multi-objective optimization in micro-electrical discharge machining using titanium nitride coated WC electrode. Int. J. Interact. Design Manuf. (IJIDeM) **17**, 187–196 (2022)
10. Rao, T.B.: Prediction of EDMed micro-hole quality characteristics using hybrid bio-inspired machine learning-based predictive approaches. Int. J. Interact. Design Manuf. (IJIDeM) (2022)
11. Dharmadhikari, S., Nikam, M., Mastud, S., Bhole, K.: Micro-fabrication of textured surfaces using wire-mesh electrode in reverse μEDM. Int. J. Interact. Design Manuf. (IJIDeM) (2023)
12. Davis, R., Singh, A., Debnath, K., Sabino, R.M., Popat, K., Soares, P., Keshri, A.K., Borgohain, B.: Enhanced micro-electric discharge machining-induced surface modification on biomedical Ti-6Al-4V alloy. J. Manuf. Sci. Eng. **144**, 12 (2021)
13. Arrabiyeh, P.A., Dethloff, M., Müller, C., Kirsch, B., Aurich, J.C.: Optimization of micropencil grinding tools via electrical discharge machining. J. Manuf. Sci. Eng. **141**, 1 (2019)
14. Viharos, Z.J., Farkas, B.Z.: Microsecond measurement resolution for process cycle diagnostics of micro-EDM milling. Meas. Sens. **18**, 100123 (2021)
15. Dutta, S., Sarma, D.K.: Multi-objective optimization of μ-EDM parameters for μ-hole drilling on Hastelloy C 276 super alloy using Response Surface Methodology and multi-objective genetic algorithm. CIRP J. Manuf. Sci. Technol. **39**, 115–133 (2022)
16. Ekmekci, B., Yaşar, H., Ekmekci, N.: A discharge separation model for powder mixed electrical discharge machining. J. Manuf. Sci. Eng. **138**, 3 (2016)
17. Valentinčič, J., Bissacco, G., Tristo, G.: Uncertainty of the electrode wear on-machine measurements in micro EDM milling. J. Manuf. Process. **64**, 153–160 (2021)
18. Pandey, A.K., Anas, M.: Sustainability and recent trends in micro-electric discharge machining (-EDM): a state-of-the-art review. Mater. Today Proc. **57**, 2049–2055 (2022)
19. Raju, L., Hiremath, S.S.: A state-of-the-art review on micro electro-discharge machining. Procedia Technol. **25**, 1281–1288 (2016)
20. Sheelwant, A., Jadhav, P.M., Narala, S.K.R.: ANN-GA based parametric optimization of Al-TiB2 metal matrix composite material processing technique. Mater. Today Commun. **27**, 102444 (2021)

21. Roy, A., Sachin, B., Raghavendra, T., Rao, C.M., Naik, G.M., Soni, H., Mashinini, P.M., Narendranath, S.: Optimizing machining responses of homologous TiNiCu shape memory alloys using hybrid ANN-GA approach. Mater. Today Proc. **62**, 4402–4410 (2022)
22. Zheng, K., Politis, D.J., Wang, L., Lin, J.: A review on forming techniques for manufacturing lightweight complex—shaped aluminium panel components. Int. J. Lightw. Mater. Manuf. **1**, 55–80 (2018)
23. Mahajan, R., Krishna, H., Singh, A.K., Ghadai, R.K.: A review on copper and its alloys used as electrode in EDM. IOP Conf. Ser. Mater. Sci. Eng. **377**, 012183 (2018)
24. Vinoth Kumar, S., Pradeep Kumar, M.: Optimization of cryogenic cooled EDM process prameters using grey relation analysis. J. Mech. Sci. Technol. **28**, 3777–3784 (2014)
25. Das, P.P., Tiwary, A.P., Chakraborty, S.: A hybrid MCDM approach for parametric optimization of a micro-EDM process. Int. J. Interact. Design Manuf. (IJIDeM) **16**, 1739–1759 (2022)
26. Kumar, L., Kumar, K., Chhabra, D.: Experimental investigations of electrical discharge micro-drilling for Mg-alloy and multi-response optimization using MOGA-ANN. CIRP J. Manuf. Sci. Technol. **38**, 774–786 (2022)
27. Joshi, A.S., Kulkarni, O., Kakandikar, G.M., Nandedkar, V.M.: Cuckoo search optimization- a review. Mater. Today Proc. **4**, 7262–7269 (2017)
28. Shanthi, S.A., Umamakeswari, T., Saranya, M.: MCDM method on complex picture fuzzy soft environment. Mater. Today Proc. **51**, 2375–2379 (2022)
29. Sharma, V., Misra, J.P., Singhal, P.: Optimization of process parameters on Combustor Material Using Taguchi & amp MCDM Method in Electro-Discharge Machining (EDM). Mater. Today Proc. **18**, 2672–2678 (2019)
30. Emovon, I., Oghenenyerovwho, O.S.: Application of MCDM method in material selection for optimal design: a review. Results Mater. **7**, 100115 (2020)